Charge screening effect in metallic carbon nanotubes

K. Sasaki*
Department of Physics, Tohoku University, Sendai 980-8578, Japan
(Received 11 December 2001; published 26 April 2002)

The charge screening effect in metallic carbon nanotubes is investigated in a model including the one-dimensional long-range Coulomb interaction. It is pointed out that an external charge which is being fixed spatially is screened by internal electrons so that the resulting object becomes electrically neutral. We found that the screening length is given by about the diameter of a nanotube.

DOI: 10.1103/PhysRevB.65.195412 PACS number(s): 73.63.Fg, 73.22.−f

I. INTRODUCTION

Recently carbon nanotubes[1] (CNTs) have attracted much attention from various points of view. Especially their unique mechanical, electrical, chemical properties have stimulated many people's interest in the analysis of CNTs.[2,3] They have exceptional strength and stability, and they can exhibit either metallic or semiconducting properties depending on the diameter and helicity.[4,5] Due to their small size, properties of CNT's should be governed by the law of quantum mechanics. Therefore it is quite important to understand the quantum behavior of electrons in CNT's.

However in a low-energy region ($<10^4$ K), we do not have to examine all electrons in the system but low-energy excitations near the Fermi level. The low energy excitations at half-filling move along the tubule axis because the circumference degree of freedom (an excitation in the compactified direction) is frozen by a wide energy gap ($\sim 10^4$ K). Hence this system can be described as a $(1+1)$-dimensional system. Furthermore, in the case of metallic CNT's, the system describing small fluctuations around the Fermi points is equivalent to the two components ''massless'' fermions in $1+1$ dimensions. This allows us to analyze the low-energy excitations with sufficient accuracy by means of a technique in quantum field theory.

Quantum-mechanical behavior of the ''massless'' fermions in metallic CNT's is governed by many kinds of interactions.[6–9] Among others the Coulomb interaction is the most important interaction and drives the system into a strongly correlated system. The purpose of this paper is to investigate how the Coulomb interaction plays the role when the system is perturbed. Particularly we try to answer the following basic question. ''What is happening when we put an external charge on a metallic carbon nanotube?'' The external charge which we consider in this paper, is externally fixed spinless particle. This is thought to be a charged impurity in a metallic nanotube.[10] To answer the above question we investigate the charging energy and charge screening effect.[11–13]

This paper is composed as follows. A model Hamiltonian for the low-energy excitations in metallic nanotubes is constructed in Sec. II. In Sec. III, we rewrite the kinetic Hamiltonian in terms of current operators. Then we examine the Hamiltonian including the long-range Coulomb interaction and analyze some effects of the Coulomb interaction on charging energy and charge screening effect in Sec. IV. In Sec. V we consider the gate-electron interaction to show the effect of the long-range Coulomb interaction against an external perturbation. Conclusion and discussion are given in Sec. VI. An other type of the Coulomb potential[8] is considered in Appendix A. We give an alternative simple derivation to obtain main results using the spin-charge separation in Appendix B.

II. THE HAMILTONIAN

Low-energy excitations in metallic carbon nanotubes consist of four independent fermion fields. Their quanta are spin-up ($\uparrow$) and -down ($\downarrow$) electrons in the K and K' Fermi points. We denote these fields as

$$\Psi_i=\begin{pmatrix}\psi_{L,i}\\ \psi_{R,i}\end{pmatrix},\quad i\in(\uparrow,\downarrow)\times(K,K'), \tag{1}$$

where i is a label for the four fermions and these fermions are expressed by $\Psi_{K_\uparrow},\Psi_{K_\downarrow},\Psi_{K'_\uparrow},\Psi_{K'_\downarrow}$, respectively. For example, the field $\Psi_{K_\uparrow}$ expresses the spin-up electron field in the K Fermi point. Hereafter we use i as an element of the set: $S=\{K_\uparrow,K_\downarrow,K'_\uparrow,K'_\downarrow\}\equiv(\uparrow,\downarrow)\times(K,K')$ as in Eq. (1). Each fermion field consists of two-component spinor, which we name $\psi_{L,i}$ and $\psi_{R,i}$. This two-component structure is due to the specific lattice structure of the graphite sheet.[14] The subscripts L and R denote left-handed component and right-handed component, respectively. The left and right are defined by the eigenvalue of the matrix $\gamma^5(=\sigma_3)$ and σ_3 is the z component of the Pauli spin matrix.

Time evolution of these fields is governed by the complicated Hamiltonian in realistic circumstances. For example, tubes are not strict straight line but generally bend[6] and the end of a tube (cap) might mix the wave functions of different Fermi points.[15] We restrict our attention to the most basic and important interactions: kinetic interaction, one-dimensional long-range Coulomb interaction and gate-electron interaction with a simple boundary condition. The kinetic term is

$$\mathcal{H}_F=\sum_{i\in S}\Psi_i^\dagger h_F\Psi_i=v_F\sum_{i\in S}\Psi_i^\dagger\begin{pmatrix}P_x & 0\\ 0 & -P_x\end{pmatrix}\Psi_i, \tag{2}$$

where $P_x=i\hbar\partial_x$ is the momentum in the tubule axis direction ($=x\in[0{:}L]\equiv D$) and v_F is the Fermi velocity. It is remarkable that the dispersion relation is linear due to the

 ©2002 The American Physical Society

special band structure of the π electrons in the graphite sheet. Therefore, we call these fermions ''massless'' fermions.

The one-dimensional long-range Coulomb interaction is

$$\mathcal{H}_C=\frac{e^2}{8\pi}\int_D \frac{J(x)J(y)}{\sqrt{|x-y|^2+d^2}}dy, \tag{3}$$

where e is the electron charge and d in the denominator denotes the diameter of a nanotube. $J(x)$ stands for the sum of each fermion charge density $J_i(x)[\equiv\Psi_i^\dagger(x)\Psi_i(x)]$,

$$J(x)=\sum_{i\in S} J_i(x). \tag{4}$$

A comment is in order regarding introducing the cutoff d in the Coulomb potential in Eq. (3). When we write the Coulomb interaction without the cutoff, it has an ultraviolet divergence in the limit of $x\to y$. To avoid the divergence, we need to introduce a cutoff. It is appropriate to set it the diameter of a tube because when two electrons on a nanotube come from opposite sides of the tubule axis direction, they repeal and pass each other. At the moment they approach most, there is still a distance about the diameter of a nanotube to decrease the energy of such event. This is an origin of the cutoff. Similar kind of cutoff[8] in the Coulomb potential is derived from integrating out the circumference degree of the Coulomb interaction. Both potentials have the same behavior at long distance scale $|x-y|\geqslant O(d)$. However there is a significant difference at short distance scale $|x-y|<O(d)$. Some detailed discussions about this potential are given in Appendix A.

We also include the effect of gate voltage on a nanotube. The interaction between the gate voltage and electrons is

$$\mathcal{H}_G=eV_gJ(x), \tag{5}$$

where V_g is a gate voltage that the massless fermions feel. It should be noted that the gate voltage is not usually equivalent to a voltage of the gate itself because of the capacitance of a substrate. We may consider the position dependent gate voltage $V_g(x)$ as a model for an electrical contact or as an external perturbation to a nanotube. Response of the system against a local gate voltage is investigated in Sec. V. By comparing the system including the long-range Coulomb interaction with the one excluding the interaction, we show how the long-range Coulomb interaction changes the response to the local gate voltage.

The microscopic Hamiltonian density for this system is

$$\mathcal{H}=\mathcal{H}_F+\mathcal{H}_C+\mathcal{H}_G. \tag{6}$$

We shall analyze this Hamiltonian without any approximation. As for the screening of an external charged particle that is being fixed on the surface of the metallic zigzag-type nanotubes and do not have a spin, we may neglect the nonlinear interactions,[8] such as the backscattering processes, because the total charge sector (B6) decouples from these interactions.

Figure 1 shows a nanotube, the perturbations that we shall analyze in the present paper, and all relevant scale of this system. The left inset (a) in Fig. 1 indicates a perturbation by an external charge that has the charge density $J_{ex}(x)$. The right inset (b) shows the interaction between a local gate (an electrical contact) and a tube. Because we model the system as one-dimensional one, we should restrict our attention to the perturbation that has the radial symmetry as is shown in both insets. However one may apply the model to a perturbation localized in radial direction providing the perturbation is weak enough.[13]

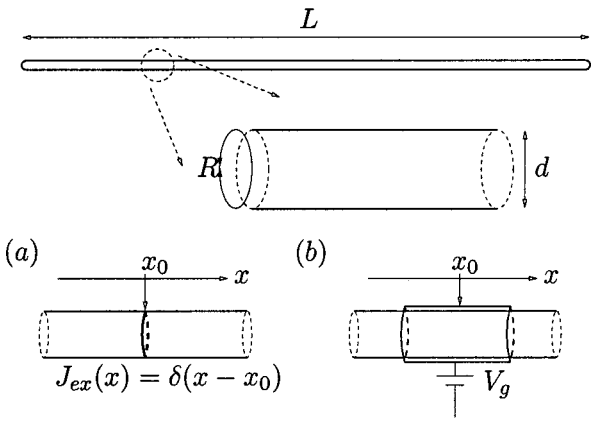

FIG. 1. The perturbations (external charge and gate-electron interaction) and all relevant scale of this system.

III. QUANTIZATION OF ELECTRON

We have specified the Hamiltonian density that describes the low-energy excitations in metallic nanotubes. In this section we quantize the massless fermion fields and rewrite the kinetic Hamiltonian in terms of the bosonic current operators.[16] The Coulomb interaction and gate-electron interaction will be investigated in later sections.

The energy eigenfunctions of the first quantized kinetic Hamiltonian are given by

$$h_F\psi_n\begin{pmatrix}1\\0\end{pmatrix}=\epsilon_n\psi_n\begin{pmatrix}1\\0\end{pmatrix}, \tag{7}$$

$$h_F\psi_n\begin{pmatrix}0\\1\end{pmatrix}=-\epsilon_n\psi_n\begin{pmatrix}0\\1\end{pmatrix}, \tag{8}$$

$$\psi_n(x)=\frac{1}{\sqrt{L}}e^{-i(\epsilon_n/\hbar v_F)x}, \tag{9}$$

where ϵ_n is the energy eigenvalues and L is the length of a metallic nanotube. The energy eigenvalues are quantized by a boundary condition. Here we impose the periodic boundary condition on the wave functions $\psi_n(x+L)=\psi_n(x)$. This boundary condition yields the following energy spectra:

$$\epsilon_n=\frac{2\pi\hbar v_F}{L}n\equiv\Delta n, \tag{10}$$

where Δ is an energy scale, which depends only on the length of a nanotube. In order to evaluate the numerical value of this energy we use the formula for the Fermi velocity

$$v_F=\frac{3\gamma a}{2\hbar}\sim\frac{c}{343}, \tag{11}$$

where c is the speed of light, $\gamma\ (=2.7eV)$ (Ref. 5) is the overlap (hopping) integral and $a\ (=1.42\ \text{Å})$ is the nearest-neighbor distance between two carbon atoms. For a single-wall nanotube with $L=3\ \mu$m, Δ is about 1.2 meV.

Each massless fermion field can be decomposed into the left- and right-handed component field as

$$\Psi_i(x,t)\equiv\Psi_{L,i}(x,t)+\Psi_{R,i}(x,t), \tag{12}$$

where t is the time. The left- and right-handed component fields consist of the energy eigenfunctions and annihilation operators of each quantum,

$$\Psi_{L,i}(x,t)=\sum_{n\in Z}a_n^i\psi_n(x)e^{-i(\epsilon_n/\hbar)t}\begin{pmatrix}1\\0\end{pmatrix}, \tag{13}$$

$$\Psi_{R,i}(x,t)=\sum_{n\in Z}b_n^i\psi_n(x)e^{+i(\epsilon_n/\hbar)t}\begin{pmatrix}0\\1\end{pmatrix}, \tag{14}$$

where a_n^i, b_n^j are independent fermionic annihilation operators of the left-handed component of the ith fermion and the right-handed component of the jth fermion satisfying the anticommutators

$$\{a_n^i,a_m^{j\dagger}\}=\{b_n^i,b_m^{j\dagger}\}=\delta^{ij}\delta_{nm}. \tag{15}$$

All of the other anticommutators vanish.

In $1+1$ dimensions, it is possible to construct the fermion Fock space by acting bosonic creation operators which are bilinear of the fermion operators on the vacuum. Because the Coulomb interaction consists of a product of the charge density, it is very convenient to rewrite the kinetic term H_F $(=\oint\mathcal{H}_F)$ using the bosonic charge density operators. For this purpose, it is useful to introduce the left and right currents as follows:

$$J(x)=J_L(x)+J_R(x). \tag{16}$$

The left and right currents for each fermion, are defined as

$$J_{L,i}(x)=\Psi_{L,i}^\dagger(x)\Psi_{L,i}(x),$$

$$J_{R,i}(x)=\Psi_{R,i}^\dagger(x)\Psi_{R,i}(x). \tag{17}$$

We expand these currents by the Fourier modes. We start with the left sector. The left current can be written as follows:

$$J_L(x)\equiv\sum_{i\in S}J_{L,i}(x)=\sum_{n\in Z}j_L^n\frac{1}{L}e^{-i(2\pi nx/L)}, \tag{18}$$

where each components are given by

$$j_L^n=\sum_{i\in S}j_{L,i}^n,\quad j_{L,i}^n=\sum_{m\in Z}a_m^{i\dagger}a_{m+n}^i,\quad j_{L,i}^0\equiv Q_{L,i}.$$

The Fourier component $j_{L,i}^n$ (current operators) satisfies the following commutation relations on the fermion Fock space (current algebra):

$$[j_{L,i}^n,(j_{L,j}^m)^\dagger]=n\delta_{ij}\delta_{nm},\quad (j_{L,i}^m)^\dagger=j_{L,i}^{-m}. \tag{19}$$

We proceed to consider the right sector in the same way. The current operators are

$$J_R(x)\equiv\sum_{i\in S}J_{R,i}(x)=\sum_{n\in Z}j_R^n\frac{1}{L}e^{+i(2\pi nx/L)}, \tag{20}$$

$$j_R^n=\sum_i j_{R,i}^n,\quad j_{R,i}^n=\sum_{m\in Z}b_{m+n}^{i\dagger}b_m^i,\quad j_{R,i}^0\equiv Q_{R,i}.$$

They satisfy the bosonic commutation relations

$$[j_{R,i}^n,(j_{R,j}^m)^\dagger]=n\delta_{ij}\delta_{nm},\quad (j_{R,i}^m)^\dagger=j_{R,i}^{-m}. \tag{21}$$

The left charge $Q_{L,i}$ and right charge $Q_{R,i}$ are conserved separately because the system is invariant under the following two independent global transformations of fermion fields, $\Psi_{L,i}\to e^{i\theta_{L,i}}\Psi_{L,i}, \Psi_{R,i}\to e^{i\theta_{R,i}}\Psi_{R,i}$. We must rewrite the fermion Hamiltonian such that all the matrix elements are the same as the original fermion Hamiltonian by means of current algebra. It is well known that the following Hamiltonian has the same matrix element as the original fermion Hamiltonian[16,17]

$$H_F=\Delta\sum_{i\in S}\left[\left(\frac{\langle Q_i\rangle^2+\langle Q_{5,i}\rangle^2}{4}-\frac{1}{12}\right)+\sum_{n>0}\{(j_{L,i}^n)^\dagger j_{L,i}^n+(j_{R,i}^n)^\dagger j_{R,i}^n\}\right], \tag{22}$$

where the $U(1)$ charge Q_i and the chiral charge $Q_{5,i}$ for each massless fermion is defined by the summation and subtraction between the left and right charges,

$$Q_i=Q_{L,i}+Q_{R,i},\quad Q_{5,i}=Q_{L,i}-Q_{R,i}. \tag{23}$$

The physical meaning of the chiral charge is spatial integration of the electric current density $ev_F[J_L(x)-J_R(x)]$ in a tube. This charge measures the left-right asymmetry of the vacuum and is defined by the difference of the left charge and the right charge on the vacuum. Note that the vacuum energy in the last equation is nonvanishing, which is due to the finite-size effect of a nanotube. Here $\langle O\rangle$ means the vacuum expectation value of an operator O. We have defined the second quantized vacuum by filling the negative-energy modes, leaving the positive-energy modes empty.

IV. LONG-RANGE COULOMB INTERACTION

The one-dimensional long-range Coulomb interaction in metallic nanotubes is given by the following potential form:

$$H_C=\int_D \mathcal{H}_C dx=\frac{e^2}{8\pi}\int\int_D \frac{J(x)J(y)}{\sqrt{|x-y|^2+d^2}}dxdy, \quad (24)$$

where d is the diameter of a nanotube and this is the trace of the pseudo-one-dimensional nature of carbon nanotubes. The total Hamiltonian of this system consists of the kinetic Hamiltonian and the Coulomb interaction. The kinetic Hamiltonian is written in terms of the current operators as is shown in the preceding section. The Coulomb interaction can also be rewritten in terms of the current operators because total charge density in the Coulomb interaction is a sum of the left and right current operators,

$$J(x)=\sum_{n\in Z}[(j_L^n)^\dagger+j_R^n]\frac{1}{L}e^{+i(2\pi nx/L)}. \quad (25)$$

Hence, by replacing $J(x)$ by Eq. (25) in the Coulomb interaction (24), we obtain

$$H_C=\frac{e^2}{8\pi L}V(0)\left(\sum_{i\in S}\langle Q_i\rangle\right)^2+\frac{e^2}{4\pi L}\sum_{n>0}V(n)[(j_L^n)^\dagger+j_R^n]\times[j_L^n+(j_R^n)^\dagger]. \quad (26)$$

We have introduced the Fourier components of the Coulomb potential as

$$V(n)=2\int_0^\pi dx\frac{\cos(2nx)}{\sqrt{x^2+\left(\frac{R}{L}\right)^2}}, \quad (27)$$

where R is the circumference ($R=\pi d$) of a nanotube. The Coulomb interaction is given by the sum of zero mode $V(0)$ and nonzero modes $V(n)$. The nonzero Fourier mode ($n\neq 0$) can be approximated to the modified Bessel function $V(n)\sim 2K_0[2n(R/L)]$ quite well if $R/L\ll 1$.

We can include external charges in the theory by replacing the total charge density J with the sum of the internal charge J and external c-number charge density J_{ex} in the Coulomb interaction

$$H_C=\frac{e^2}{8\pi}\int\int_D \frac{[J(x)+J_{ex}(x)][J(y)+J_{ex}(y)]}{\sqrt{|x-y|^2+d^2}}dxdy. \quad (28)$$

It is straightforward to derive the corresponding expression in terms of current operators

$$H_C=\frac{e^2}{8\pi L}V(0)\left(\sum_{i\in S}\langle Q_i\rangle+J_{ex}\right)^2+\sum_{n>0}\beta_n[(j_L^n)^\dagger+j_R^n+(j_{ex}^n)^*][j_L^n+(j_R^n)^\dagger+j_{ex}^n], \quad (29)$$

where we introduce $\beta_n\equiv(e^2/4\pi L)V(n)$ and define the Fourier components of the external charge as follows:

$$J_{ex}(x)=\frac{1}{L}\sum_{n\in Z}j_{ex}^n e^{-i(2\pi nx/L)}. \quad (30)$$

Total charge of the external particle is given by the spatial integration of the c-number external charge density which is referred to Q_{ex},

$$Q_{ex}\equiv\int_D J_{ex}(x)dx=j_{ex}^0. \quad (31)$$

We finally obtain the long-range Coulomb interaction in terms of the current operators, which modifies the energy spectra of the original kinetic Hamiltonian that we discussed in the preceding section. Before we analyze the total Hamiltonian quantum mechanically, it is important to know the order of magnitude of the long-range Coulomb interaction. Typical energy scale of the Coulomb interaction (β_n) of this system is strong as compared with the energy scale of the kinetic interaction. This is shown by the ratio of the energy scale of the Coulomb interaction to the energy separation of the kinetic interaction

$$\frac{\beta_n}{\Delta}=\frac{\alpha}{\pi}\frac{c}{v_F}K_0\left(2n\frac{R}{L}\right), \quad (32)$$

where $\alpha(\equiv e^2/4\pi\hbar c\sim\frac{1}{137})$ is the fine-structure constant. We used the approximation formula $V(n)\sim 2K_0[2n(R/L)]$ in Eq. (32). The value of the ratio is more than 1 for $n\leqslant O(L/2R)$. Therefore this system is thought to be a strongly correlated system. So, we should first estimate the Coulomb energy scale of the physical quantities in this system. For this purpose, we treat the Coulomb interaction roughly in Sec. IV A. A detailed analysis of the system will be given in latter section.

A. Order estimation

When an externally fixed particle with total charge Q_{ex} is put on a metallic nanotube, the charge density of the particle may be modeled by the δ function,

$$J_{ex}(x)=Q_{ex}\delta(x-x_0), \quad (33)$$

where we put the particle at $x_0(\in[0{:}L])$. It can be thought that this external charge distribution is a model for a charged spinless impurity.

It is important to estimate the order of magnitude of the energy that we need to put a fixed external charge on a metallic nanotube. We simply neglect the interaction between internal electrons and the external charge, so we set $\langle J(x)\rangle=0$. In this case, we get

$$\langle H_C\rangle=\frac{e^2}{8\pi}\int\int_D\frac{J_{ex}(x)J_{ex}(y)}{\sqrt{|x-y|^2+d^2}}dxdy=\frac{e^2}{8\pi}\frac{1}{d}Q_{ex}^2. \quad (34)$$

Estimation of this value for a metallic nanotube with $d=1.4$ nm gives $\langle H_C\rangle\sim 515Q_{ex}^2$ meV. As is discussed in the following section, this energy is strongly modified by the Coulomb interaction between internal electrons and the external charge. The internal electrons move or rearrange in order to decrease the energy of the system. This means that the charge screening effect occurs.

On the other hand, in an experiment concerning transport on nanotubes, an electron flows from the electric contact and after some period it spreads uniformly in a nanotube. Then we have

$$J_{ex}(x)=Q_{ex}\frac{1}{L}. \tag{35}$$

In this case, the Coulomb self-energy is

$$\langle H_C\rangle=\frac{e^2}{8\pi}\frac{1}{L}\ln\left[\frac{\sqrt{1+\left(\frac{d}{L}\right)^2}+1}{\sqrt{1+\left(\frac{d}{L}\right)^2}-1}\right]Q_{ex}^2\sim\frac{e^2}{4\pi}\frac{1}{L}\ln\left(\frac{2L}{d}\right)Q_{ex}^2. \tag{36}$$

For a metallic nanotube with $d=1.4$ nm and $L=3.2$ μm, we obtain $\langle H_C\rangle\sim 3.8Q_{ex}^2$ meV. It should be noticed that Eq. (36) is the same formula that is usually used in the analysis of the Coulomb blockade phenomena of a transport experiment of nanotubes. This energy is called ''charging energy (E_c)'' and is not modified by the interaction with internal charges due to its uniform distribution,

$$E_c\equiv\frac{e^2}{4\pi}\frac{1}{L}\ln\left(\frac{2L}{d}\right). \tag{37}$$

An experimental value of the charging energy for a metallic single-wall CNT with $d+1.4$ nm and $L=3.2$ μm in length is about $E_c=3.8$ meV (Ref. 18) and is very close to the above estimation. This is a verification of the cutoff in the potential of the Coulomb interaction.

B. Screening effect

We have so far considered the long-range Coulomb interaction very roughly. In this section we solve the system quantum mechanically and examine the charge screening effect. To investigate this effect, we shall compute the charging energy and induced charge distribution by an external charge. We start with one massless fermion case. This case corresponds to an approximation that we only consider the system with one massless fermion, for example, $\Psi_{K_\uparrow}$. Four massless fermions case (metallic nanotubes case) can be obtained by straightforward extension of the one massless fermion case.

1. One fermion case

The total Hamiltonian is given by

$$H=\Delta\left\{\left(\frac{\langle Q\rangle^2+\langle Q_5\rangle^2}{4}-\frac{1}{12}\right)+\sum_{n>0}\left[(j_L^n)^\dagger j_L^n+(j_R^n)^\dagger j_R^n\right]\right\}$$
$$+E_c(\langle Q\rangle+Q_{ex})^2+\sum_{n>0}\beta_n[(j_L^n)^\dagger+j_R^n+(j_{ex}^n)^*]$$
$$\times[j_L^n+(j_R^n)^\dagger+j_{ex}^n], \tag{38}$$

where we omit the subscript i because we consider one massless fermion case. The kinetic term and the Coulomb term can be combined as follows:

$$H=H_0-\frac{\Delta}{12}+\sum_{n>0}H_n, \tag{39}$$

where

$$H_0=\frac{\Delta}{4}[\langle Q\rangle^2+\langle Q_5\rangle^2]+E_c(\langle Q\rangle+Q_{ex})^2, \tag{40}$$

$$H_n=\Delta[(j_L^n)^\dagger j_L^n+(j_R^n)^\dagger j_R^n]+\beta_n[(j_L^n)^\dagger+j_R^n+(j_{ex}^n)^*]$$
$$\times[j_L^n+(j_R^n)^\dagger+j_{ex}^n]. \tag{41}$$

H_0 is the zero mode Hamiltonian whose structure is simple and is already diagonalized. Hereafter we choose the vacuum with vanishing $U(1)$ charge $(\langle Q\rangle=0)$ and the chiral charge $(\langle Q_5\rangle=0)$ for simplicity. In this case we have $H_0=E_cQ_{ex}^2$. We diagonalize the Hamiltonian $H_n(n\neq 0)$ using the Bogoliubov transformation of the current operators

$$\begin{pmatrix}\tilde{j}_L^n\\(\tilde{j}_R^n)^\dagger\end{pmatrix}=\begin{pmatrix}\cosh t_n & \sinh t_n\\ \sinh t_n & \cosh t_n\end{pmatrix}\begin{pmatrix}j_L^n\\(j_R^n)^\dagger\end{pmatrix}, \tag{42}$$

where

$$\sinh 2t_n=\frac{\beta_n}{E_n},\quad \cosh 2t_n=\frac{1}{E_n}(\Delta+\beta_n),$$
$$E_n=\Delta\sqrt{1+\frac{2\beta_n}{\Delta}}.$$

The Bogoliubov transformed currents $(\tilde{j}_L^n,\tilde{j}_R^n)$ satisfy the same bosonic commutation relations as the original current operators (19) and (21),

$$[\tilde{j}_L^n,(\tilde{j}_L^m)^\dagger]=[\tilde{j}_R^n,(\tilde{j}_R^m)^\dagger]=n\,\delta_{nm}. \tag{43}$$

After some calculations we diagonalize H_n as follows:

$$H_n=E_n[\{(\tilde{j}_L^n)^\dagger+\gamma_n(j_{ex}^n)^*\}(\tilde{j}_L^n+\gamma_n j_{ex}^n)+\{(\tilde{j}_R^n)^\dagger+\gamma_n j_{ex}^n\}$$
$$\times\{\tilde{j}_R^n+\gamma_n(j_{ex}^n)^*\}+n]-\Delta n+\beta_n\frac{\Delta^2}{E_n^2}(j_{ex}^n)^*j_{ex}^n, \tag{44}$$

where $\gamma_n=\sinh 2t_n(\cosh t_n-\sinh t_n)$. It is easy to find conditions of the vacuum $|\mathrm{vac}_1;J_{ex}\rangle$ in the presence of the external charges (''vac_1'' in the ket denotes vacuum state for the ''one'' massless fermion),

$$(\tilde{j}_L^n+\gamma_n j_{ex}^n)|\mathrm{vac}_1;J_{ex}\rangle=0,$$
$$(\tilde{j}_R^n+\gamma_n(j_{ex}^n)^*)|\mathrm{vac}_1;J_{ex}\rangle=0,\quad n>0. \tag{45}$$

We estimate the energy change between the two vacua

$|\mathrm{vac}_1;0\rangle$ (without an external charge) and $|\mathrm{vac}_1;J_{ex}\rangle$ (with an external charge)

$$\delta E=\langle \mathrm{vac}_1;J_{ex}|H(J_{ex})|\mathrm{vac}_1;J_{ex}\rangle-\langle \mathrm{vac}_1;0|H(0)|\mathrm{vac}_1;0\rangle$$

$$=E_cQ_{ex}^2+\sum_{n>0}\beta_n\frac{\Delta^2}{E_n^2}(j_{ex}^n)^*j_{ex}^n$$

$$=E_cQ_{ex}^2+\sum_{n>0}\frac{\beta_n}{1+\dfrac{2\beta_n}{\Delta}}(j_{ex}^n)^*j_{ex}^n, \tag{46}$$

where $H(J_{ex})$ denotes the Hamiltonian with the external charge distribution J_{ex}. If we neglect the Coulomb interaction between the internal charges and the external charge, as in the preceding section, the charging energy is given by

$$E_cQ_{ex}^2+\sum_{n>0}\beta_n(j_{ex}^n)^*j_{ex}^n. \tag{47}$$

Comparing this with the exact result (46) one can recognize the difference between these results. The effect of internal charge redistribution enters in the denominator of second term in Eq. (46). Therefore if the energy separation of the kinetic spectrum is huge compared with the Coulomb interaction,

$$\frac{\beta_n}{\Delta}\ll 1, \tag{48}$$

the effect of rearrangement of the internal electrons is very small so that the charging energy is hardly modified from the previous order estimation. However for metallic nanotubes, the situation is completely different as we have mentioned at Eq. (32).

Next, let us consider the rearrangement of the internal electrons. This rearrangement can be shown in the expectation value of the charge density operator,

$$J(x)=\sum_{n\in Z}((j_L^n)^\dagger+j_R^n)\frac{1}{L}e^{+i(2\pi nx/L)}$$

$$=\frac{Q}{L}+\sum_{n>0}\sqrt{\frac{\Delta}{E_n}}[(\tilde{j}_L^n)^\dagger+\tilde{j}_R^n]\frac{1}{L}e^{+i2\pi nx/(L)}$$

$$+\sum_{n>0}\sqrt{\frac{\Delta}{E_n}}[\tilde{j}_L^n+(\tilde{j}_R^n)^\dagger]\frac{1}{L}e^{-i(2\pi nx/L)}. \tag{49}$$

The expectation value can be calculated using the definition of the vacuum in the presence of the external charge (45),

$$\langle J(x)\rangle_1\equiv\langle \mathrm{vac}_1;J_{ex}|J(x)|\mathrm{vac}_1;J_{ex}\rangle$$

$$=\sum_{n>0}\sqrt{\frac{\Delta}{E_n}}(-2\gamma_n)\frac{1}{L}$$
$$\times[(j_{ex}^n)^*e^{+i(2\pi nx/L)}+j_{ex}^ne^{-i(2\pi nx/L)}]$$

$$=\sum_{n>0}-\frac{\dfrac{2\beta_n}{\Delta}}{1+\dfrac{2\beta_n}{\Delta}}\frac{1}{L}$$
$$\times[(j_{ex}^n)^*e^{+i(2\pi nx/L)}+j_{ex}^ne^{-i(2\pi nx/L)}]. \tag{50}$$

For the δ-function charge distribution (33), we obtain

$$\langle J(x)\rangle_1=Q_{ex}\sum_{n>0}-\frac{\dfrac{2\beta_n}{\Delta}}{1+\dfrac{2\beta_n}{\Delta}}\frac{2}{L}\cos\left[\frac{2\pi n}{L}(x-x_0)\right]. \tag{51}$$

2. Two fermion case

Let us proceed to the two fermions case. Here we use $i=\{1,2\}$ instead of, for example, $i=\{K_\uparrow,K_\downarrow\}$ for simplicity. Even in the two fermions case zero mode sector of the Hamiltonian is very simple and it gives only the charging energy $E_cQ_{ex}^2$. We should diagonalize the nonzero modes of the Hamiltonian. This part is given as follows:

$$H_n=\Delta[(j_{L,1}^n)^\dagger j_{L,1}^n+(j_{R,1}^n)^\dagger j_{R,1}^n]+\Delta[(j_{L,2}^n)^\dagger j_{L,2}^n+(j_{R,2}^n)^\dagger j_{R,2}^n]$$
$$+\beta_n[(j_{L,1}^n)^\dagger+j_{R,1}^n+(j_{L,2}^n)^\dagger+j_{R,2}^n+(j_{ex}^n)^*]$$
$$\times[j_{L,1}^n+(j_{R,1}^n)^\dagger+j_{L,2}^n+(j_{R,2}^n)^\dagger+j_{ex}^n]. \tag{52}$$

First we focus on the fermion labeled by 1. If we regard $j_{L,2}^n+(j_{R,2}^n)^\dagger+j_{ex}^n$ as j_{ex}^n in the previous analysis, we get the following expression instead of Eq. (44)

$$H_n=E_n(\{(\tilde{j}_{L,1}^n)^\dagger+\gamma_n[(j_{L,2}^n)^\dagger+j_{R,2}^n+(j_{ex}^n)^*]\}(\tilde{j}_{L,1}^n+\gamma_n[j_{L,2}^n$$
$$+(j_{R,2}^n)^\dagger+j_{ex}^n])+\{(\tilde{j}_{R,1}^n)^\dagger+\gamma_n[j_{L,2}^n+(j_{R,2}^n)^\dagger+j_{ex}^n]\}$$
$$\times\{\tilde{j}_{R,1}^n+\gamma_n[(j_{L,2}^n)^\dagger+j_{R,2}^n+(j_{ex}^n)^*]\}+n)-\Delta n$$
$$+\Delta[(j_{L,2}^n)^\dagger j_{L,2}^n+(j_{R,2}^n)^\dagger j_{R,2}^n]+\beta_n\frac{\Delta^2}{E_n^2}[(j_{L,2}^n)^\dagger+j_{R,2}^n$$
$$+(j_{ex}^n)^*][j_{L,2}^n+(j_{R,2}^n)^\dagger+j_{ex}^n], \tag{53}$$

The last two lines in the above equation have almost same structure as the one that we have analyzed in the preceding section, Eq. (41). However in the present case, the Coulomb interaction term is modified as follows:

$$\beta_n\to\beta_n\frac{\Delta^2}{E_n^2}. \tag{54}$$

We use the same method (Bogoliubov transformation) to diagonalize this part of the Hamiltonian with rotation angle s_n which is different from the previous one (t_n).

$$\begin{pmatrix} \tilde{j}^n_{L,2} \\ (\tilde{j}^n_{R,2})^\dagger \end{pmatrix} = \begin{pmatrix} \cosh s_n & \sinh s_n \\ \sinh s_n & \cosh s_n \end{pmatrix} \begin{pmatrix} j^n_{L,2} \\ (j^n_{R,2})^\dagger \end{pmatrix}, \tag{55}$$

where

$$\sinh 2s_n = \frac{\beta_n \frac{\Delta^2}{E_n^2}}{F_n}, \cosh 2t_n = \frac{1}{F_n}\left(\Delta + \beta_n \frac{\Delta^2}{E_n^2}\right),$$

$$F_n = \Delta \sqrt{1 + \frac{2\beta_n}{\Delta}\frac{\Delta^2}{E_n^2}}.$$

This transformation gives the result which is similar to Eq. (44),

$$F_n[\{(\tilde{j}^n_{L,2})^\dagger + \delta_n (j^n_{ex})^*\}(\tilde{j}^n_{L,2} + \delta_n j^n_{ex}) + \{(\tilde{j}^n_{R,2})^\dagger + \delta_n j^n_{ex}\} \times \{\tilde{j}^n_{R,2} + \delta_n (j^n_{ex})^*\} + n] - \Delta n + \beta_n \frac{\Delta^2}{E_n^2}\frac{\Delta^2}{F_n^2}(j^n_{ex})^* j^n_{ex}, \tag{56}$$

where $\delta_n = \sinh 2s_n(\cosh s_n - \sinh s_n)$. We define the vacuum for the two fermion case with the external charge distribution.

$$(\tilde{j}^n_{L,2} + \delta_n j^n_{ex})|\mathrm{vac}_2; J_{ex}\rangle = 0,$$

$$\{\tilde{j}^n_{R,2} + \delta_n (j^n_{ex})^*\}|\mathrm{vac}_2; J_{ex}\rangle = 0,$$

$$\{\tilde{j}^n_{L,1} + \gamma_n[j^n_{L,2} + (j^n_{R,2})^\dagger + j^n_{ex}]\}|\mathrm{vac}_2; J_{ex}\rangle = 0,$$

$$\{\tilde{j}^n_{R,1} + \gamma_n[(j^n_{L,2})^\dagger + j^n_{R,2} + (j^n_{ex})^*]\}|\mathrm{vac}_2; J_{ex}\rangle = 0.$$

From Eqs. (53), (56) and the above definitions of the vacuum, the energy change of the two vacua $|\mathrm{vac}_2; 0\rangle$ and $|\mathrm{vac}_2; J_{ex}\rangle$ is evaluated as

$$\delta E = E_c Q_{ex}^2 + \sum_{n>0} \beta_n \frac{\Delta^2}{E_n^2}\frac{\Delta^2}{F_n^2}(j^n_{ex})^* j^n_{ex}$$

$$= E_c Q_{ex}^2 + \sum_{n>0} \frac{\beta_n}{1 + 2\frac{2\beta_n}{\Delta}}(j^n_{ex})^* j^n_{ex}. \tag{57}$$

We see that the effect of ''two'' fermions on the charging energy is the factor 2 in front of the $2\beta_n/\Delta$ in the denominator of second term. This means that the charging energy decreases more as compared with the one fermion case. On the other hand, the internal electron charge density distribution becomes

$$\langle J(x)\rangle_2 = \sum_{n>0} -\frac{2\frac{2\beta_n}{\Delta}}{1 + 2\frac{2\beta_n}{\Delta}}\frac{1}{L}[(j^n_{ex})^* e^{+i(2\pi nx/L)} + j^n_{ex} e^{-i(2\pi nx/L)}]. \tag{58}$$

It can be seen that the effect of the two fermions on the induced charge density is also the factor 2 in front of the $2\beta_n/\Delta$ terms.

3. Four fermion case

A Four fermion case can be analyzed by the same procedure as the two fermions case. The calculation is straightforward but lengthy, so we shall omit it here. Instead, we give an alternative simple derivation in Appendix. B. The formulas for the charging energy and induced internal charge density are

$$\delta E = E_c Q_{ex}^2 + \sum_{n>0} \frac{\beta_n}{1 + \frac{8\beta_n}{\Delta}}(j^n_{ex})^* j^n_{ex}, \tag{59}$$

$$\langle J(x)\rangle_4 = \sum_{n>0} -\frac{\frac{8\beta_n}{\Delta}}{1 + \frac{8\beta_n}{\Delta}}\frac{1}{L}[(j^n_{ex})^* e^{+i(2\pi nx/L)} + j^n_{ex} e^{-i(2\pi nx/L)}], \tag{60}$$

where the subscript 4 of the vacuum expectation value ($\langle J(x)\rangle_4$) indicates the vacuum of the four fermion case. Notice that these equations can be obtained from the results of the one fermion case by replacing the level spacing as follows:

$$\Delta \to \frac{\Delta}{4}. \tag{61}$$

For the δ-function charge distribution of the external charge (33), we obtain

$$\delta E = \left[E_c + \sum_{n>0} \frac{\beta_n}{1 + \frac{8\beta_n}{\Delta}}\right] Q_{ex}^2, \tag{62}$$

$$\langle J(x)\rangle_4 = Q_{ex} \sum_{n>0} -\frac{\frac{8\beta_n}{\Delta}}{1 + \frac{8\beta_n}{\Delta}}\frac{2}{L}\cos\left(\frac{2\pi n}{L}(x - x_0)\right). \tag{63}$$

The numerical value of the above charging energy is about $85Q_{ex}^2$ meV for a metallic nanotube with $d = 1.4$ nm and $L = 3$ μm. This value is to be compared with the previous estimation of the Coulomb self-energy of the external charge $\langle H_C\rangle \sim 515 Q_{ex}^2$ meV in Eq. (34). This indicates that many internal electrons are influenced by the external charge and

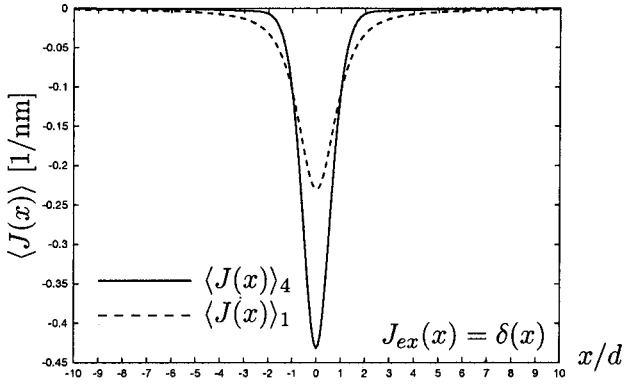

FIG. 2. Position dependence of the induced charge density in the presence of an external spinless point particle (33) that has unit charge $Q_{ex}=1$. The screening length reaches several d (diameter of a nanotube). The solid line is given by the formula of the four fermion case (63), the dashed line is for the one fermion case (51). This dashed line corresponds to the week coupling case ($\alpha/4$) of the four fermion case. We used $d=1.4$ nm and $L=3$ μm in these plots.

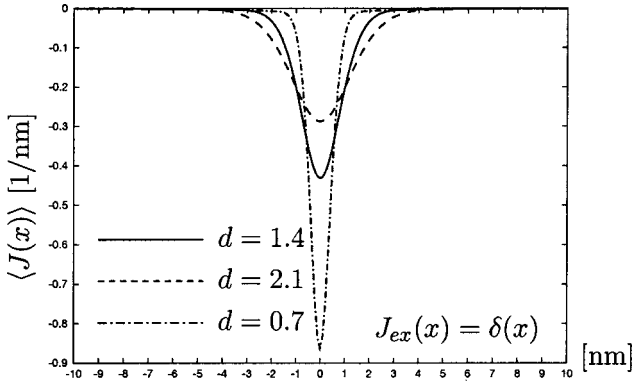

FIG. 3. Diameter dependence of the screening length. The scale of the length is given by nanometer unit. The solid line is for $d=1.4$ nm metallic nanotube, the dashed line is for $d=2.1$ nm case, and the dashed-dotted line is for $d=0.7$ nm. We use $L=3$ μm and $Q_{ex}=1$ in these plots.

rearranged. To confirm this we plot the expectation value of the internal charge density in Fig. 2.

Notice that the induced charge density spreads within the range of $O(d)$.[13] This fact can be recognized by the following reason. In Eq. (63), we may approximately regard the summation over n by integral of $a\equiv 2n(R/L)$ if the length of a nanotube is huge compared with the circumference ($R/L \ll 1$). This gives

$$Q_{ex}\int_{0^+}^{\infty} -\frac{8\frac{\alpha}{\pi}\frac{c}{v_F}K_0(a)}{1+8\frac{\alpha}{\pi}\frac{c}{v_F}K_0(a)}\frac{1}{R}\cos\left(a\frac{x-x_0}{d}\right)da. \quad (64)$$

Therefore a remaining typical length scale is the diameter of a nanotube. Therefore the length of the nanotubes has only small dependece on the screening effect. Off course, the screening length depends on the physical parameter such as the coupling constant of the Coulomb interaction (α) and the Fermi velocity. We also plot Eq. (51) of the one fermion case. The equation corresponds to the week coupling ($\alpha \to \alpha/4$) of the four fermion case. The screening length is related to a cutoff in the long-range Coulomb interaction, then if we take another type of cutoff, the screening length depends on it.

Let us consider nanotubes having different diameters. Figure 3 shows the induced charge distribution (63) for nanotubes with $d=0.7$,1.4, and 2.1 nm. Here we suppose that these nanotubes have the same length $L=3$ μm. It should be noted that the screening length is proportional to the diameter of a nanotube.

V. GATE-ELECTRON INTERACTION

In this section we consider the position dependent gate voltage and discuss the effect of the Coulomb interaction between the internal electrons in this system. The gate voltage is expanded in a Fourier series

$$V_g(x)=g\sum_{n\in Z} v_g^n e^{-i(2\pi nx/L)}, \quad (65)$$

where g has the dimension of voltage. In this case the gate-electron interaction consists of the zero mode and nonzero modes

$$H_G=egv_g^0Q+\sum_{i\in S}\sum_{n>0} eg[v_g^n(j_{L,i}^n)^\dagger+(v_g^n)^*j_{L,i}^n] + eg[v_g^n j_{R,i}^n+(v_g^n)^*(j_{R,i}^n)^\dagger]. \quad (66)$$

Let us concentrate on the nonzero modes of the one fermion case without an external charge. The Hamiltonian for the nonzero modes is rewritten as

$$H_n=E_n[\{(\tilde{j}_L^n)^\dagger+\Gamma_n(v_g^n)^*\}(\tilde{j}_L^n+\Gamma_n v_g^n)+\{(\tilde{j}_R^n)^\dagger+\Gamma_n v_g^n\} \times\{\tilde{j}_R^n+\Gamma_n(v_g^n)^*\}+n]-\Delta n-2E_n\Gamma_n^2(v_g^n)^*v_g^n, \quad (67)$$

where

$$\Gamma_n=\frac{eg}{E_n}\sqrt{\frac{\Delta}{E_n}}. \quad (68)$$

The above Hamiltonian gives us definitions of the vacuum,

$$(\tilde{j}_L^n+\Gamma_n v_g^n)|\mathrm{vac}_1;V_g\rangle=0,$$

$$[\tilde{j}_R^n+\Gamma_n(v_g^n)^*]|\mathrm{vac}_1;V_g\rangle=0, \quad n>0. \quad (69)$$

With these definitions we compute the expectation value of the charge density operator. As a simple example, we use a local gate potential, which has the Gaussian form

$$V_g(x)\sim g\sqrt{\frac{k}{\pi}}e^{-k(x-x_0)^2}, \quad v_g^n\sim e^{-\pi^2n^2/kL^2}e^{i(2\pi nx_0/L)}, \quad (70)$$

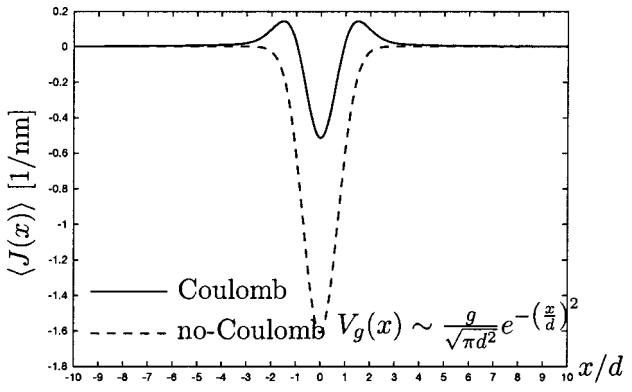

FIG. 4. Position dependence of the induced charge density by the local gate voltage (70). The solid line is given by the formula (71) and the dashed line is given by the same formula however without the Coulomb interaction ($\beta_n=0$). We set $2eg/\Delta=1$ for a metallic nanotube with $d=1.4$ nm and $L=3$ μm.

where k decides the size of the local gate potential. Here we set $k=1/d^2$. This gives the induced charge density for the four fermion case,

$$\langle J(x)\rangle_4 = -\sum_{n>0} \frac{4\frac{2eg}{\Delta}}{1+4\frac{2\beta_n}{\Delta}} \frac{2}{L} e^{-(R/L)^2 n^2} \cos\left(\frac{2\pi n}{L}(x-x_0)\right). \tag{71}$$

In order to see the effect of the long-range Coulomb interaction on the induced charge density, we plot this function with the Coulomb interaction and without it ($\beta_n=0$) in Fig. 4. The plots in Fig. 4 show that the long-range Coulomb interaction between the internal electrons significantly changes the response of the system to the external perturbation. The effect of the Coulomb interaction on the induced charge density appears in the denominator of the above result. It should be noted that the finite width of the local gate voltage makes the effective range of n in the summation small and the high frequency modes of the potential ineffective.

VI. DISCUSSION AND COMMENTS

In this paper we have analyzed the charge screening effect in metallic carbon nanotubes. The significance of our present work is as follows.

We modeled the Hamiltonian (6) describing the low-energy excitations in metallic nanotubes and solved the system in the presence of the external charge and the local gate voltage. It was found that when we put an external particle on a metallic nanotube, the electric charge of the particle is screened by internal electrons due to the long-range Coulomb interaction between the particle and the internal electrons. The Coulomb interaction is strong as compared with the energy scale of the kinetic Hamiltonian (32). This fact makes the quantum-mechanical screening complete.

The screening length is given by about the diameter of a nanotube in regard to the long-range Coulomb potential (24). However the length depends on the cutoff in the potential of the Coulomb interaction (see Appendix A), therefore it is important to understand the short distance behavior of the potential to find more accurate value of the screening length. This is a nontrivial problem because the short distance corresponds to the high-energy region, hence we necessarily examine other bands in addition to the linear bands. Anyway the effective range of screening (about the diameter of a nanotube or less than that) is very small compared with the length of a nanotube, the end of a nanotube (cap) can be thought to be ineffective to the screening phenomena.

The formula for the induced charge density in the presence of a point particle is given by Eq. (63). The summation over n in this equation converges due to Eq. (32). Due to this an extra cutoff of n is not necessary.[14] In substance the summation converges up to $n\sim O(L/d)$. However, the high-frequency modes $[n>O(L/d)]$ of the long-range Coulomb interaction might be influenced by the other bands that do not belong to the ''massless'' dispersion bands. We would like to make a quantitative analysis of these ''massive'' bands in a future report.

ACKNOWLEDGMENTS

The author would like to thank T. Ando and A. Farajian for fruitful discussion. This work was supported by the Japan Society of the Promotion of Science.

APPENDIX A

We may use another kind of the long-range Coulomb potential which is derived from integrating out the circumference degree of the Coulomb interaction with a cutoff a_z.[8] The interaction is given by

$$H_C = \frac{e^2}{8\pi} \int \int_D J(x) V(x-y) J(y) dx dy \tag{A1}$$

with the potential

$$V(x) = \frac{1}{\sqrt{|x|^2+d^2+a_z^2}} \frac{2}{\pi} K\left(\frac{d}{\sqrt{|x|^2+d^2+a_z^2}}\right). \tag{A2}$$

$K(z)$ is the complete elliptic integral of the first kind and the cutoff $a_z(\sim a)$ denotes the average distance between a $2p_z$ electron and the nucleus. It should be noted that a new length scale a_z in addition to L(length of a nanotube) and d(diameter) is coming out. This scale modifies the behavior of the potential at short distance $(x\to 0)$ as is shown in Fig. 5.

Hence Fourier components of the potential

$$V(n) = \frac{2}{\pi} \int_0^{\frac{\pi}{2}} 2K_0\left[2n\frac{R}{L}\sqrt{\sin^2 x + \left(\frac{a_z}{d}\right)^2}\right] dx \tag{A3}$$

are different from the previous one $V(n)\sim 2K_0[2n(R/L)]$. We plot the induced charge density using Eq. (A3) in Fig. 6. It can be seen that the screening length is about one-half of the length of the diameter.

It is important to note that the effective range of n summation in the formula of the induced charge density becomes

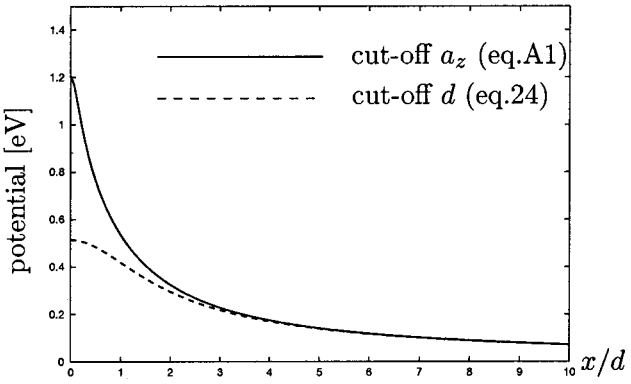

FIG. 5. Position dependence of the Coulomb potentials. The solid line is given by the formula (A1) and the dashed line is the potential that we used in the text. Here we take $d=1.4$ nm and $a_z=1.4$ Å.

large compared with the Coulomb interaction in the text. Within this plot, the summation converges up to $n\sim O(L/\pi a_z)$. So, it is not clear whether the screening effect can be recognized in the framework of the ''low-energy'' excitations. In order to answer such question, we introduce a regulator to examine if the high-frequency modes of the potential give a significant contribution to the final result.[14] Here we take a simple regulator

$$\mathrm{reg}(n)=\frac{1}{\exp[n-n^*]+1}, \tag{A4}$$

where $n^*\sim O(L/d)$. We define the following induced charge density:

$$\langle J(x)\rangle_4^{\mathrm{reg}}\equiv\sum_{n>0}-\frac{\mathrm{reg}(n)\dfrac{8\beta_n}{\Delta}}{1+\dfrac{8\beta_n}{\Delta}}\frac{2}{L}\cos\left(\frac{2\pi n}{L}(x-x_0)\right). \tag{A5}$$

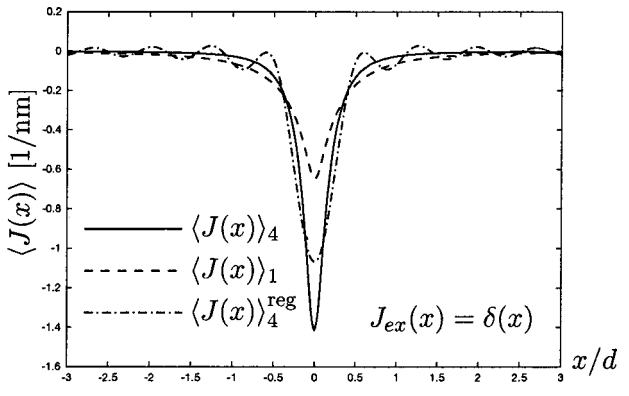

FIG. 6. Position dependence of the induced charge density by an external spinless point particle (33) with $Q_{ex}=1$. The solid line is given by the formula for the four fermion case (63), the dashed line is for the one fermion case (44). The dotted-dashed line shows the function in Eq. (A5) that is regularized by the function (A4) with $n^*=3000\sim O(L/d)$. We use the Fourier components (A3) and take $a_z=1.4(\sim a)$ Å, $d=1.4$ nm and $L=3$ μm in these plots.

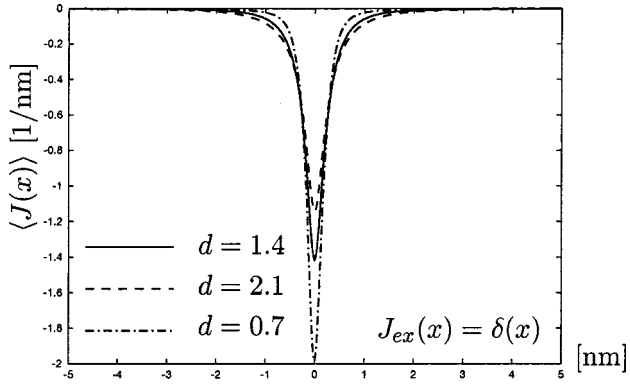

FIG. 7. Diameter dependence of the screening length. The scale of the length is given in nanometers. The solid line is for $d=1.4$ nm metallic nanotube, the dashed line is for $d=2.1$ nm case, and the dashed-dotted line is for $d=0.7$ nm. We use the Fourier components (A3) and take $a_z=1.4(\sim a)$ Å and $L=1$ μm in these plots.

This function is also shown in Fig. 6. We see from this figure that the induced charge density oscillates. This is due to the regulator and does not have any physical meaning. What needs to be emphasized at this point is that the screening effect arises from the contribution of the low-energy region $n<n^*$. Thus it is concluded that the charge screening can be analyzed in the low-energy physics.

Let us consider nanotubes having different diameters. Figure 7 shows the induced charge distribution for nanotubes with $d=0.7,1.4,2.1$ nm by means of the Coulomb potential (A2). Here we suppose that these nanotubes have the same length $L=1$ μm. It should be noted that the screening length is proportional to the diameter of a nanotube. However as compared with the previous potential case (Fig. 3), the diameter dependence is rather weak.

APPENDIX B

Here we derive the final results, Eq. (59) and (60), using the operator decomposition into spin and charge. First we consider the density operator for K Fermi point. We define the following operators for the K point:

$$J_{L,C_K}=J_{L,K_\uparrow}+J_{L,K_\downarrow},$$

$$J_{L,S_K}=J_{L,K_\uparrow}-J_{L,K_\downarrow}, \tag{B1}$$

where we omit spatial dependence of these operator for simplicity and J_{L,C_K},J_{L,S_K} express the charge and spin operators of left-handed fermions in the K Fermi point. Similarly for the right-handed sector at K Fermi point, we define

$$J_{R,C_K}=J_{R,K_\uparrow}+J_{R,K_\downarrow},$$

$$J_{R,S_K}=J_{R,K_\uparrow}-J_{R,K_\downarrow}. \tag{B2}$$

The commutation relations between these operators can be calculated by using the commutation relation of original operators $(J_{L,i},J_{R,i})$. For example, we obtain the following commutation relation:

$$[J_{L,C_K}(x),J_{L,C_K}(y)]=2\frac{i}{2\pi}\partial_x\delta(x-y). \tag{B3}$$

For K' Fermi point, similarly we define

$$J_{L,C_{K'}}=J_{L,K'_\uparrow}+J_{L,K'_\downarrow},J_{L,S_{K'}}=J_{L,K'_\uparrow}-J_{L,K'_\downarrow},$$

$$J_{R,C_{K'}}=J_{R,K'_\uparrow}+J_{R,K'_\downarrow},J_{R,S_{K'}}=J_{R,K'_\uparrow}-J_{R,K'_\downarrow}.$$

Using above definitions of the density operators, we define the symmetric and antisymmetric combination concerning two Fermi points using the above spin and charge operators for the left-handed sector as follows:

$$J_{L,C_+}=J_{L,C_K}+J_{L,C_{K'}},J_{L,C_-}=J_{L,C_K}-J_{L,C_{K'}},$$

$$J_{L,S_+}=J_{L,S_K}+J_{L,S_{K'}},J_{L,S_-}=J_{L,S_K}-J_{L,S_{K'}}.$$

Similarly for the right-handed sector

$$J_{R,C_+}=J_{R,C_K}+J_{R,C_{K'}},J_{R,C_-}=J_{R,C_K}-J_{R,C_{K'}},$$

$$J_{R,S_+}=J_{R,S_K}+J_{R,S_{K'}},J_{R,S_-}=J_{R,S_K}-J_{R,S_{K'}}.$$

We get the following kinetic Hamiltonian in terms of these new density operators

$$\begin{aligned}H_F=&\Delta\left[\frac{L}{8}\int_D:J_{L,C_+}(x)^2+J_{R,C_+}(x)^2:dx-\frac{1}{12}\right]\\&+\Delta\left[\frac{L}{8}\int_D:J_{L,C_-}(x)^2+J_{R,C_-}(x)^2:dx-\frac{1}{12}\right]\\&+\Delta\left[\frac{L}{8}\int_D:J_{L,S_+}(x)^2+J_{R,S_+}(x)^2:dx-\frac{1}{12}\right]\\&+\Delta\left[\frac{L}{8}\int_D:J_{L,S_-}(x)^2+J_{R,S_-}(x)^2:dx-\frac{1}{12}\right].\end{aligned}$$

Let us define the following operator and this is actually equivalent to the charge density operator,

$$J_{C_+}=J_{L,C_+}+J_{R,C_+}, \tag{B4}$$

$$J(x)=J_{C_+}(x). \tag{B5}$$

Therefore we find that the total charge sector is decoupled from other operators and this is the famous spin and charge separation in one-dimensional systems. The Coulomb interaction is written only by the total charge density. Hence we combine the kinetic term and the long-range Coulomb term and define C_+ sector as follows:

$$\begin{aligned}H_{C_+}\equiv&\Delta\left[\frac{L}{8}\int_D:J_{L,C_+}(x)^2+J_{R,C_+}(x)^2:dx-\frac{1}{12}\right]+\frac{e^2}{8\pi}\\&\times\int\int_D\frac{[J_{C_+}(x)+J_{ex}(x)][J_{C_+}(y)+J_{ex}(y)]}{\sqrt{|x-y|^2+d^2}}dxdy.\end{aligned} \tag{B6}$$

This Hamiltonian is very similar to the one fermion case that we have analyzed. The current operator is defined in the same way as in the preceding section

$$J_{C_+}(x)=\sum_{n\in Z}[(j^n_{L,C_+})^\dagger+j^n_{R,C_+}]\frac{1}{L}e^{+i(2\pi nx/L)}. \tag{B7}$$

Notice that the commutation relation is modified

$$[J_{L,C_+}(x),J_{L,C_+}(y)]=4\frac{i}{2\pi}\partial_x\delta(x-y), \tag{B8}$$

and we obtain the current algebra

$$[j^n_{L,C_+},(j^m_{L,C_+})^\dagger]=4n\delta_{nm}, \tag{B9}$$

$$[j^n_{R,C_+},(j^m_{R,C_+})^\dagger]=4n\delta_{nm}. \tag{B10}$$

Analysis of the above Hamiltonian can be done simular to the one fermion case. We decompose it into zero mode and nonzero modes,

$$H_{C_+}=H_0-\frac{\Delta}{12}+\sum_{n>0}H_n, \tag{B11}$$

where

$$H_0=\frac{\Delta}{16}[\langle Q\rangle^2+\langle Q_5\rangle^2]+E_c(\langle Q\rangle+Q_{ex})^2 \tag{B12}$$

$$\begin{aligned}H_n=&\frac{\Delta}{4}[(j^n_{L,C_+})^\dagger j^n_{L,C_+}+(j^n_{R,C_+})^\dagger j^n_{R,C_+}]+\beta_n[(j^n_{L,C_+})^\dagger\\&+j^n_{R,C_+}+(j^n_{ex})^*]\times[j^n_{L,C_+}+(j^n_{R,C_+})^\dagger+j^n_{ex}].\end{aligned} \tag{B13}$$

We can get this Hamiltonian by the following replacement in the one fermion Hamiltonians (40) and (41), see also Eq. (61),

$$\Delta\to\frac{\Delta}{4}. \tag{B14}$$

Therefore formulas of the charging energy and induced charge density for the four fermion case can be obtained by the above replacement in the equations, which was obtained in the analysis of the one fermion case.

*Email address: sasaki@tuhep.phys.tohoku.ac.jp

[1] S. Iijima, Nature (London) **354**, 56 (1991).

[2] R. Saito, G. Dresselhaus, and M.S. Dresselhaus, *Physical Properties of Carbon Nanotubes* (Imperial College Press, London, 1998).

[3] C. Dekker, Phys. Today **52**, 22 (1999).

[4] J.W. Mintmire, B.I. Dunlap, and C.T. White, Phys. Rev. Lett. **68**, 631 (1992); N. Hamada, S. Sawada, and A. Oshiyama, *ibid.* **68**, 1579 (1992); R. Saito *et al.*, Appl. Phys. Lett. **60**, 2204 (1992).

[5] J.W.G. Wildöer *et al.*, Nature (London) **391**, 59 (1998); T.W. Odom *et al.*, *ibid.* **391**, 62 (1998).

[6] C.L. Kane and E.J. Mele, Phys. Rev. Lett. **78**, 1932 (1997).
[7] C. Kane, L. Balents, and M.P.A. Fisher, Phys. Rev. Lett. **79**, 5086 (1997).
[8] R. Egger and A.O. Gogolin, Phys. Rev. Lett. **79**, 5082 (1997); Eur. Phys. J. B **3**, 281 (1998).
[9] H. Yoshioka and A.A. Odintsov, Phys. Rev. Lett. **82**, 374 (1999).
[10] H. Ajiki and T. Ando, Solid State Commun. **102**, 135 (1997); T. Ando and T. Nakanishi, J. Phys. Soc. Jpn. **67**, 1704 (1998).
[11] A.A. Farajian, K. Esfarjani and Y. Kawazoe *et al.*, Phys. Rev. Lett. **82**, 5084 (1999).
[12] F. Leonard and J. Tersoff, Phys. Rev. Lett. **83**, 5174 (1999); A.A. Odintsov, *ibid.* **85**, 150 (2000).
[13] M.F. Lin and D.S. Chuu, Phys. Rev. B **56**, 4996 (1997).
[14] D.P. DiVincenzo and E.J. Mele, Phys. Rev. B **29**, 1685 (1984).
[15] T. Yaguchi and T. Ando, J. Phys. Soc. Jpn. **70**, 1327 (2001); **70**, 3641 (2001).
[16] S. Tomonaga, Prog. Theor. Phys. **5**, 544 (1950); J.M. Luttinger, J. Math. Phys. **4**, 1154 (1963); D.C. Mattis and E.H. Lieb, *ibid.* **6**, 304 (1965).
[17] S. Iso and H. Murayama, Prog. Theor. Phys. **84**, 142 (1990).
[18] H. Postma, Z. Yao, and C. Dekker J. Low Temp. Phys. **118**, 495 (2000).